One-Dimensional Numerical Simulation of Two-Fluid Nonequilibrium Plasma Flow in MPD Thrusters

Nobuyuki FUKUOKA*, Takeshi MIYASAKA†and Toshi FUJIWARA‡
Department of Aerospace Engineering,
Nagoya University
Furo-cho Chikusa-ku, Nagoya, 464-8603, Japan

Abstract

A numerical analysis of one-dimensional flow in an MPD thruster has been done, including nonequilibrium ionization/recombination processes of the propellant gas and velocity slip between charged and neutral particles. The calculated results are noticeably different from that of one-fluid model. The velocity of charged particles near the inlet is much higher than the mean velocity calculated by one-fluid model, and the inlet electron temperature of two-fluid model is much lower than that of one-fluid model. As a result, more realistic current distribution is obtained.

Introduction

Self-field MPD(magnetoplasmadynamic) thrusters are promising as a future propulsion system from a viewpoint of high specific impulse. Experiments on MPD thrusters have been performed by numerous workers[1-3]. The existing experiments explains that the current distribution in a discharge chamber is closely related to the thruster performance. In order to examine the distribution and thrust performance, numerical simulations have been done by assuming one-fluid plasma[2-8]. The calculated results for Ar show that current distributions have peaks near inlet and outlet. However, small currents are measured near the inlet in the experiments[3]. For the purpose of analyzing more realistic flows, the studies based on two-fluid models has been performed[9,10].

In this paper, numerical analyses of a two-fluid plasma flow are done, including nonequilibrium ionization/recombination processes of the propellant gas and velocity slip between charged particles and neutral particles. In this two-fluid model, ions and neutrals have different flow velocities because in an MPD thruster ions are pushed by the Lorentz force and neutrals are pushed by collisions with ions. Flow velocity of ions has special effect on current density profile, so that thrust performance of MPD is influenced by ions velocity. When mass flow rate of propellant gas becomes lower, or total discharge current becomes higher, the difference between the two flow velocity would be larger, thus the two-fluid model is important in those conditions.

In this model, the propellant gas is Argon and a heat conduction model is included. In numerical analysis of one-dimensional plasma flow in MPD, the sonic condition must be applied. Since there are two flows of ions and neutrals in this model, two sonic conditions exist. In this code the calculation of the flowfield and the electromagnetic field are performed independently. The flowfield is calculated with a 2nd-order-accurate explicit MUSCL TVD scheme, whereas the corresponding electromagnetic field is obtained by solving steady electromagnetic solutions.

Assumptions

For the purpose of simplification, the following assumptions are introduced into the present analysis:
1) The propellant gas is Argon.
2) Only the single-ionization and recombination processes are considered:

$$\mathrm{Ar} + e^- \rightleftharpoons \mathrm{Ar}^+ + e^- + e^- \ . \qquad (1)$$

3) The plasma is a perfect gas having constant specific heats.
4) The magnetic field is entirely self-induced.
5) The plasma flows one-dimensionaly.
6) The charged and neutral particles velocities are different.
7) The plasma has three different temperatures, electron, ion and neutral temperatures.
8) Only the heat conduction is considered as transport phenomena.

Fundamental Equations

Fundamental equations of flowfield

The analysis is based on the one-dimensional two-fluid equations that are written in a conservational form as

*Graduate sutudent. Currently, Toyoda Automatic !! !! !! Loom Works Ltd., Japan.
†Research associate
‡Professor, Member AIAA

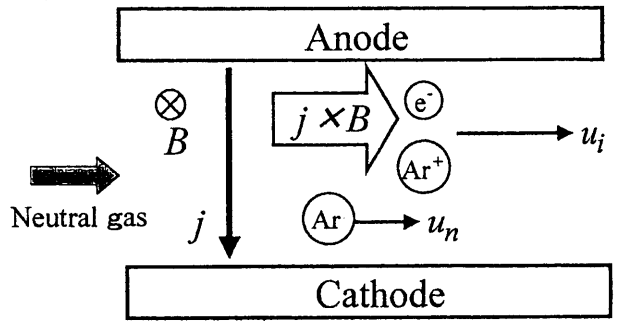

Fig. 1. Two-fluid model in MPD thrusters.

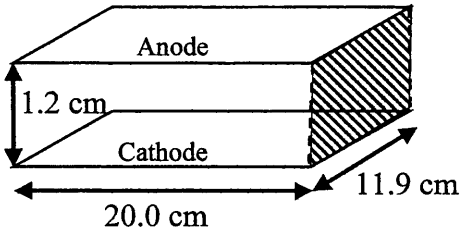

Fig. 2. Thruster configuration.

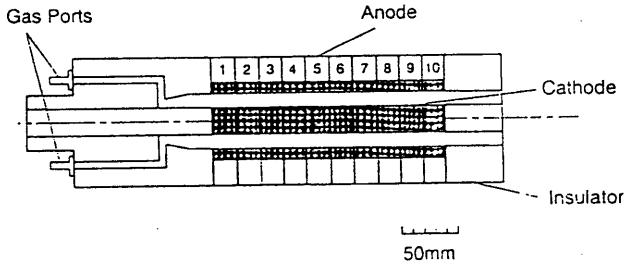

Fig. 3. Cross section of quasi-steady MPD arc channel MC-II used for referred experiment[3].

$$\frac{\partial \mathbf{U}}{\partial t} + \frac{\partial \mathbf{F}}{\partial x} = \mathbf{S} + \mathbf{H},$$

$$\mathbf{U} = \begin{bmatrix} \rho_n \\ \rho_i \\ \rho_n u_n \\ \rho_i u_i \\ e_n \\ e_i \\ e_e \end{bmatrix}, \mathbf{F} = \begin{bmatrix} \rho_n u_n \\ \rho_i u_i \\ \rho_n u_n^2 + p_n \\ \rho_i u_i^2 + p_i + p_e \\ (p_n + e_n) u_n \\ (p_i + e_i) u_i \\ e_e u_i \end{bmatrix},$$

$$\mathbf{S} = \begin{bmatrix} -\dot{\rho}_i \\ \dot{\rho}_i \\ -\dot{m}_i \\ jB + \dot{m}_i \\ -\dot{e}_i \\ jBu_i + \dot{e}_i \\ \frac{j^2}{\sigma} - \epsilon_i \dot{n}_i \end{bmatrix},$$

$$\mathbf{H} = \begin{bmatrix} 0 \\ 0 \\ F_{in} \\ -F_{in} \\ F_{in}u + Q_{en} + Q_{in} + \frac{\partial}{\partial x}\lambda_n \frac{\partial T_n}{\partial x} \\ -F_{in}u + Q_{ei} - Q_{in} - u_i \frac{\partial p_e}{\partial x} + \frac{\partial}{\partial x}\lambda_i \frac{\partial T_i}{\partial x} \\ -Q_{en} - Q_{ei} - p_e \frac{\partial u_i}{\partial x} + \frac{\partial}{\partial x}\lambda_e \frac{\partial T_e}{\partial x} \end{bmatrix}, \quad (2)$$

where

$$e_n = \frac{1}{2}\rho_n u_n^2 + \frac{p_n}{\gamma - 1}, \quad (3)$$

$$e_i = \frac{1}{2}\rho_i u_i^2 + \frac{p_i}{\gamma - 1}, \quad (4)$$

$$e_e = \frac{p_e}{\gamma - 1}. \quad (5)$$

In the equations, the subscript n represents the neutral, i the ions, e the electrons respectively. The pressure of j-species p_j is given as

$$p_j = \rho_j R_j T_j. \quad (6)$$

The values in the vectors S and H are given as follows. The rate of production $\dot{\rho}_i$ is given by the difference between ionization and recombination as

$$\dot{\rho}_i = m_g \dot{n}_f - m_g \dot{n}_b \quad (7)$$

where

$$\dot{n}_f = k_f n_i n_n, \quad \dot{n}_b = k_b n_i^3. \quad (8)$$

The rate of coefficient for ionization reaction k_f is conventionally expressed in the form:

$$k_f = \frac{76.8}{T_e^3} \exp\left(-\frac{\epsilon}{kT_e}\right), \quad (9)$$

while the rate coefficient for recombination reaction k_b is given as

$$k_b = 4.0 \times 10^{-21} T_e^{-\frac{9}{2}}. \quad (10)$$

The rate of ion momentum production by ion production $\dot{m}_i$ is given as

$$\dot{m}_i = m_g u_n \dot{n}_f - m_g u_i \dot{n}_b \quad (11)$$

and the rate of ion energy production $\dot{e}_i$ is given as

$$\dot{e}_i = \frac{e_n}{n_n}\dot{n}_f - \frac{e_i}{n_i}\dot{n}_b. \quad (12)$$

The momentum transfer F_{in} is given by

$$F_{in} = \frac{1}{2} m_g (u_i - u_n) n_i \nu_{in}. \quad (13)$$

The energy transfer from ions to neutral particles $F_{in}u$ is given by

$$F_{in}u = \frac{1}{2} m_g (u_i - u_n) n_i \nu_{in} u \quad (14)$$

where u is the mean velocity defined as

$$u = \frac{\rho_n u_n + \rho_i u_i}{\rho_n + \rho_i}. \quad (15)$$

The energy interaction between j-species and k-species Q_{jk} is given by

$$Q_{jk} = \frac{3m_j}{m_k} n_j k(T_j - T_k)\nu_{jk}. \quad (16)$$

Fundamental equations of electromagnetic field

The equations describing the electromagnetic field are written as

$$j = \sigma(E - u_i B), \quad (17)$$

$$\frac{dB}{dx} = -\mu_0 j. \quad (18)$$

Numerical Analysis

Numerical Procedure

Time-integration of the flowfield is done by using a 2nd-order- accurate explicit MUSCL TVD-upwind scheme[15], whereas the electromagnetic field is given by the steady electromagnetic equations. The time-integration proceeds until the time-dependent flowfield calculation converges to a steady solution. The calculation sequence of plasma flow is shown in Fig. 4.

Inlet Conditions

The inlet physical properties needed for the calculation are densities ρ_n, ρ_i, velocities u_n, u_i, temperatures T_n, T_i, T_e, and electric field E. The condtitions for determination of these eight properties are

1) Given discharge current J,
2) Given mass flow rate $\dot{m}$,
3) Subsonic character,
4) Sonic condition for charged particles,
5) Sonic condition for neutral particles,
6) Fixed stagnation temperature $T_0 = 300$ K,
7) Fixed inlet temperature of neutral $T_n = 300$ K,
8) Fixed inlet temperature of ions $T_i = 300$ K.

At the inlet boundary, the flow is assumed as subsonic and there are two sonic conditions of charged and neutral particles downstream as discussed in next section. Therefore, three of properties should be determined from downstream. In the present work, inlet velocities u_n, u_i, and ion temperature T_i are determined from downstream by the 1st-order extrapolation. Then we alter inlet ionization fraction α until T_i coincides 300 K. Using this α, u_n and u_i, ρ_n and ρ_i are obtained for a given mass flow rate. T_e is determined from the condition that stagnation temperature T_0 =300 K using the following equation,

$$\left[\frac{\gamma}{\gamma-1}\frac{k}{m_g}(\rho_n T_n + \rho_i T_i + \rho_i T_e) + \epsilon_i \dot{n}_i + \frac{1}{2}\rho_n u_n^2 + \frac{1}{2}\rho_i u_i^2\right]/(\rho_n u_n + \rho_i u_i) = \frac{\gamma}{\gamma-1}\frac{k}{m_g}T_0. \quad (19)$$

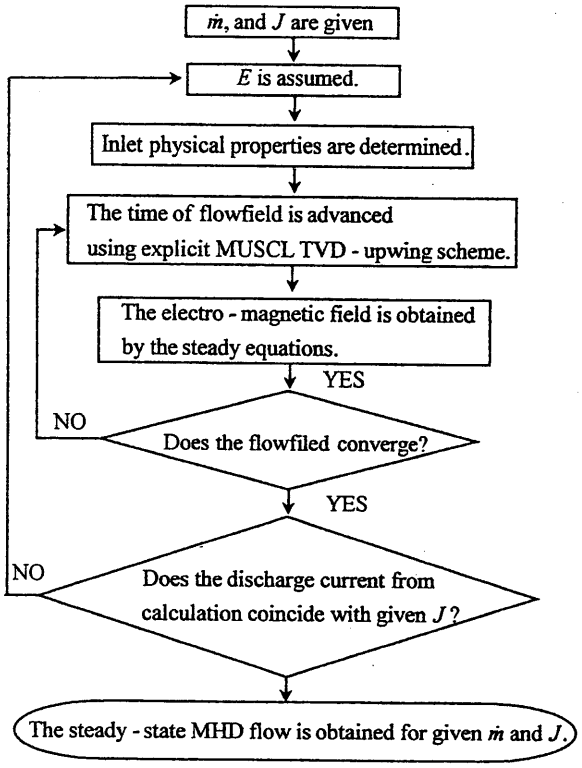

Fig. 4. Calculation sequence of plasma flow in MPD thrusters.

The only property of electromagnetic field E is determined from given discharge current J.

Sonic Conditions

Because the two-fluid model is considered in this work, there are two different sonic conditions for charged particles and neutral particles[10-13]. From the conservation equations of one-dimensional flowfield,

$$\frac{d\rho u}{dx} = X \quad (20)$$

$$\frac{d}{dx}(\rho u^2 + p) = Y \quad (21)$$

$$\frac{d}{dx}\left(\frac{1}{2}\rho u^3 + \frac{\gamma}{\gamma-1}pu\right) = Z \quad (22)$$

the velocity gradient is obtained as

$$\frac{du}{dx} = -\frac{\gamma-1}{M^2-1}\frac{1}{a^2}\left(Z - \frac{\gamma}{\gamma-1}uY + \frac{\gamma+1}{\gamma-1}\frac{u^2}{2}X\right), \quad (23)$$

where

$$M \equiv \frac{u}{a}, \quad a \equiv \gamma\frac{p}{\rho}. \quad (24)$$

In order to get continuous solution at a sonic point $M = 1$ in Eq.(23) , the denominator on the right hand of Eq.(23) should be equal to zero. Therefore, the sonic conditions for charged particles and neutral particles are given as follows.

1) Sonic condition for charged particles:
At M_i =1, we have

$$E = \frac{\gamma}{\gamma-1}\frac{u_i}{j}(jB - F_{in} + \dot{m}_i) + \frac{1}{j}(F_{in} + Q_{en} + Q_{in} + \epsilon_i \dot{n}_i - \dot{e}_i - \frac{(\gamma+1)\dot{\rho}_i u_i^2}{2(\gamma-1)j}. \quad (25)$$

2) Sonic condition for neutral particles
At M_n =1, we have

$$\frac{1}{2}\frac{\gamma+1}{\gamma-1}\dot{\rho}_i u_n^2 + \frac{\gamma}{\gamma-1}u_n(F_{in} - \dot{m}_i) - (F_{in}u + Q_{en} + Q_{in} - \dot{e}_i) = 0, \quad (26)$$

where

$$M_i \equiv \frac{u_i}{a_i}, \quad (27)$$

$$M_n \equiv \frac{u_n}{a_n}, \quad (28)$$

$$a_i^2 \equiv \gamma\frac{p_i + p_e}{\rho_i}, \quad (29)$$

$$a_n^2 \equiv \gamma\frac{p_n}{\rho_n}. \quad (30)$$

Downstream Conditions

At the downstream boundary, each property is extrapolated from the adjacent innner point, due to its supersonic character.

Results

Numerical Results are given for a fixed J(=8.1 kA) and different $\dot{m}$. These parameters along with the geometric parameters are given in Fig. 2. The parameters are chosen to be as close as possible to the referred experiment[3] (see Fig. 3).

Analyses of flowfield

Calculated properties are shown in Figs. 5-10. For the purpose of comparison between the one-fluid and two-fluid models, calculated properties of one-fluid model are also shown in Figs. 5, 8-10. Figure 5 shows the distributions of flow velocities of charged and neutral particles for $\dot{m}$ = (a) 0.481 g/s and (b) 0.368 g/s. The velocity of charged particles increases rapidly by Lorentz force near the inlet where the ionization fraction is low(see Fig. 6). Thus, the velocity is much higher than the velocity of neutral particles and mean velocity of one-fluid model in this region. The velocity difference between the charged and neutral particles remains to the downstream end. Figure 5 also explains that the difference becomes stronger for a lower mass flow rate.

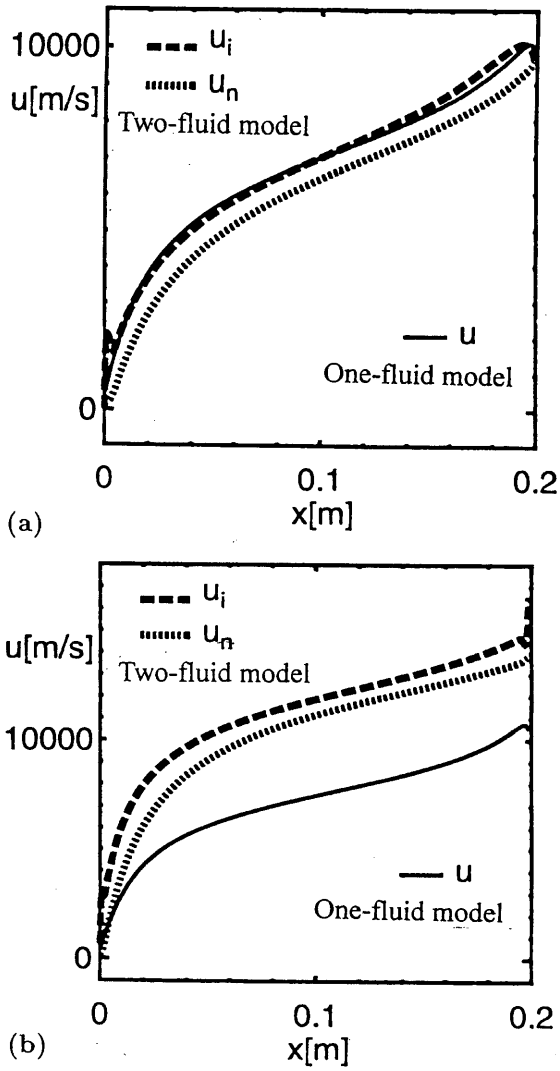

Fig. 5. Distribution of velocities of two-fluid model and mean velocity of one-fluid model for $\dot{m}$= (a) 0.481 g/s and (b) 0.368 g/s.

Figure 7 shows the distribution of temperatures of electrons, ions, and neutral particles for $\dot{m}$ =0.481 g/s. There is a noticeable difference among these three temperatures. The temperatures of ions and electrons increases rapidly downward from the inlet. Figures 8 and 9 shows the temperature of heavy particles and that of electrons respectively. The temperatures of heavy particles of two-fluid and one-fluid models differ strongly in Fig. 8. In contrast, there is not clear difference between the temperatures of electrons of two-fluid and one-fluid models except the inlet values in Fig. 9. The inlet temperature of electrons of two-fluid model is much lower than that of one-fluid.

As a result of introduction of two-fluid model, the acceleration of charged particles becomes strong near the inlet and the inlet temperature of electrons decreases remarkably. Because the current distribution depends strongly on the velocity